Conference Proceedings

Solar World Congress 2015
Daegu, Korea, 08 – 12 November 2015

Solar Thermal Reduction of Metal Oxides as a Promising Way of Converting CSP into Clean Electricity on demand

I. Vishnevetsky*

Weizmann Institute of Science, Rehovot (Israel)

Abstract

Available main results of full endothermic reduction of different metal oxides with promising for solar thermochemical redox cycles for hydrogen production and electricity generation on demand are compared. New experimental results of preliminary non solar and solar tests related to an influence of such process parameters as the partial pressure of product gases, the rate of heating and cooling, temperature of metal vapours deposit sites on the morphology and purity of reduced metals, apparent kinetic parameters, undesired by-products formation and intensity of reoxidation are discussed. It is shown that pure reduced metals with strong metal-oxygen bond strength as aluminum and magnesium can be obtain in vacuum with fast preheating rate 150-200 degree per minute with temperatures and CO partial pressure at deposit sites no higher than 460-600°C and 0.07-0.1 mbar. Morphology of such reduced metals also strongly depends on deposit temperatures and can vary from conglomerates composed of submicron and nanocrystallines (50-60°C at water cooling deposit site), metallic flakes with spherical or flat micron and submicron particles (200°C about) to metallic plates (400-600°C). The main positive and negative results of different oxides reduction are described and promising ways of future desirable investigations are proposed.

Keywords: *metal oxides, reduction, solar thermal, clean electricity, CSP, accumulation of solar energy*

1. Introduction

The main challenge of solar energy industrial application is not stable DNI that strongly depends on time of day and year and whether conditions. So processes, which allow using on demand metals reduced periodically during sunny weather, are promising. Such metals accumulate significant amount of solar energy during the endothermic reduction step followed by the exothermic oxidation step of thermochemical redox cycle when this energy can be directly converted into electricity using the metal-air fuel cells or transferred to hydrogen fuel in the hydrolysis reaction. The main problems of hydrogen energetics are storage and transportation of hydrogen fuel. Here reduced metals can be transported to a place of electricity production on demand where hydrogen will be produced close to a fuel cell on a vehicle board or near other autonomous sources of heat and power.

Last 15-20 years R&D of solar redox cycles for hydrogen and electricity production attracts a considerable interest that reflects in a significant amount of publications Reviews of such investigations were presented by Fletcher (2001), Steinfeld and Palumbo (2001), Kodama (2003), Steinfeld (2005), Roeb M. et al. (2012) and Muhich C. et al. (2015). Features of solar thermochemical redox cycles for hydrogen production from water as a function of reactants' main characteristics were described by Vishnevetsky et al. (2011). Reduction step can be oriented to full or partial reduction especially for metals with higher valence. Partial reduction or splitting usually produces suboxides in a solid phase and need lower temperatures but demonstrates lower hydrogen productivity per unit mass of solid and usually suitable for continuous hydrogen production in a solar plant cyclically with reduction step (Hydrosol project; Konstandopoulos and Agrofiotis, 2006; Scheffe and Steinfeld, 2014), It does not solve the problems related to hydrogen storage and transportation especially at a solar plant area with concentrated optics. So only full reduction, that provides higher productiveness of redox cycle for hydrogen production and electricity on demand will be considerate here.

Before solar reactor design not solar tests help to realize preliminary investigation of forward, backward reactions and morphology of reduced metals at more stable than solar conditions. Not solar setups based on conventional electrical devices must be designed to simulate different heating and cooling facilities typical for solar reactors. Three possible options of preliminary not solar reactors were described by Vishnevetsky et al. (2005, 2010, 2011b).

First one provides one side heating usually typical for solar reactor. Thermal energy here spreads in the radial direction from the SiC tube, heated by an electric current till 400 A. Such reactor was used for forward reaction investigation when the main products are vapour of a reduced metal, CO and small amount of CO_2. Reaction progress leads to layerwise volatilization of reaction mixture described by Osinga et al.(2004) as shrinking packed bed.

doi:10.18086/swc.2015.04.23 Available at http://proceedings.ises.org

The second one imitates a solar tubular reactor (see Fig, 3d below) where a cylindrical electrical furnace simulates 2D-CPC. This reactor is used for reduction of metals with boiling point higher then reaction temperature when product appears in liquid phase and does not leave the reaction zone. Morphology of the reduced metal depends on the solidification conditions and will be discussed below.

The third one, presented in the experimental section (Fig.6), provides fast heating that especially important for reaction with complicated chemistry in order to avoid by-product formation during preheating. Wide range of temperature distribution on metal vapour deposit sites in IH reactor (Vishnevetsky et al., 2013) allows investigating not only forward but also backward reaction as function of temperature at deposit sites.

Solar thermal chemical reactors for full metal oxides reduction through thermal decomposition or carbothermic reduction are available today not only at laboratory but also at a pilot scale. They can be operated at atmospheric pressure and in vacuum condition. The progress achieved during last 15 years is widely presented in the literature.

Laboratory and pilot scales of a ‘‘rotating-cavity’’ solar reactors for the thermal dissociation of ZnO were developed in PSI and ETH, Switzerland. Continuously injected ZnO powder is distributed on the rotating inner cylindrical wall, accumulates solar flux and protects cavity wall from overheating. Such reactors can provide forward reaction temperature till 2300 K. The first 10 kW version was presented by Haueter et al. (1999) and the modernized version by Schunk et al. (2008). Dynamic modelling and 100 kW pilot scale demonstration were described by Villasmil et al. (2014a, 2014b) and by Meier, (www.stage-ste.eu). Smaller 1kW solar reactor with a rotating cavity, continuously injected ZnO particles and hemispherical glass window was developed in Processes, Materials, and Solar Energy Laboratory (PROMES-CNRS), France and described by Abanades et al. (2007).

One of the main technological challenges of window solar reactors is reliable protection of quartz window from reduced metal vapour deposition. One of such way to protect flat windows is creating vortex-type stable flow with significant flow rate of carrier gas which is induced toward the aperture, similar to a tornado flow configuration proposed by Kogan and Kogan (2002). Other way to protect window is two cavity reactor developed in PSI and ETH, Switzerland. 5 kW laboratory scale reactor was described in details by Wieckert et al. (2004) and Osinga et al. (2004a, 2004b). 300 kW pilot scale was presented by Wieckert et al. (2007). Its possible industrial futures proposed by Epstein et al. (2008). The main principle of two cavity reactor is heating of reaction mixture not by direct CSP but by secondary radiation from the solar absorber placed in the upper cavity which prevents the penetration of metal vapours to the quartz window from the lower cavity where reaction can be proceed at 1500 K. Such reactors can be used for batch tests and for continues feed operation. Testing of international SOLZINC 300 kW pilot scale batch reactor with packed bad mixture of ZnO with beech charcoal was tested in Solar Research Facility Unit of WIS, Israel, using beam down optic and biggest CPC in the Wold.

Presented ways of window protections do not solve this problem completely especially during a long continuous operation of a reactor. The other way is non-windowed solar reactors developed in WIS, Israel. Such reactors can be tubular (Adinberg and Epstein, 2004) or with ceramic crucible (Vishnevetsky et al., 2006). Here SiC ceramic parts (tubes or crucibles) are sealed and irradiated with indirect or direct CSP. Advanced SiC ceramics as Hexoloy SA, for example, must possess superior strength characteristics and high working temperature to withstand the high temperature gradient from the colder flange for safe sealing to the hot reaction zone. Such 30 kW laboratory scale reactors were tested in the WIS Solar Tower using parabolic mirror and CPC as second and third concentrators after heliostats.

Light elements with strong metal oxygen bond strength need very high temperature for carboreduction of their oxides at atmospheric pressure. As it is well known according Le Chatelier’s principle vacuum conditions can reduce significantly temperatures of such reactions but need additional energy consumption for pumping. Different energy and temperature estimations as function of pressure were presented by Vishnevetsky and Epstein (2015). This 10 kW vacuum solar reactor was developed and tested in WIS, Israel, and presented below in Fig.7. Stoichiometric reaction mixture (a few tens of grams) of oxides with beach charcoal was compressed to pellets 1 cm diameter using 10wt.% of sugar as a binder. The main test results obtained during magnesia, alumina and boria solar carboreduction in vacuum are presented by Vishnevetsky et al. (2012, 2013, 2014, 2015). According preliminary investigation a sharp temperature drop from the hot reaction zone to the deposit site is necessary in order to avoid the recombination during metal vapor deposotion. So design of this vacuum reactor with spherical quartz window was accompanied by numerical simulation of temperatures and stress distribution (Vishnevetsky et al., 2012, Ben-Zvi, 2013), that was confirmed by good resistance of the quartz window during tests and measuring temperature values which changed from 1900 K in the reaction zone till 320 K about at water cooling deposit site. This reactor was modified later by adding the second option as uncooled deposit area to study vapour deposition at higher temperature for getting liquid reduced metal.

Miniature (1g reactant) solar vacuum reactor was also developed and tested in CNRS-PROMES, France (Abanades et al., 2008 and Chambon et al., 2010).

New available solar and not solar test results are presented below. It includes effecting of such process parameters as the partial pressure of product gases, the rate of heating and cooling, temperature of metal vapours deposit sites on the

morphology of reduced metals, on apparent kinetic parameters, undesired by-products formation and intensity of reoxidation. The main challenges and possible ways to avoid these problems also will be discussed.

2. Thermodynamics

The main equations of thermochemical redox cycle for full oxides reduction are thermal carboreduction (Eq.1a) or thermolysis (Eq.1b) followed by hydrolysis (Eq.2) or oxidation in metal-air fuel cells (Eq.3) of fully reduced metals:

$$Me_xO_y + yC = xMe + yCO \quad \text{(eq.1a)}$$

$$Me_xO_y = xMe + \left(\frac{y}{2}\right)O_2 \quad \text{(eq.1b)}$$

$$xMe + yH_2O = Me_xO_y + yH_2 \quad \text{(eq.2)}$$

$$xMe + 0.5yO_2 = Me_xO_y \quad \text{(eq.3)}$$

Partial reduction of oxides can be realized for metals with higher valence at lower temperatures, but it is not considered here as hydrolysis/oxidation of suboxides have lower productiveness.

As it is well known the reaction summarized in Eq.1a is not solid-solid reaction (Berman amd Epstein, 1999; Byung-Su Kim et all., 2006) but gas-solid reaction ($Me_xO_y+yCO=xMe+yCO_2$) with intermediate gas product CO_2. Depending on the reaction temperature, CO_2 is fully or partially transformed to CO through the Boudouard reaction ($C+CO_2=2CO$). For carboreduction processing at atmospheric pressure Boudouard reaction usually is responsible for the reaction rate. Full conversion of CO_2 to CO occurs at 1100 -1200°C or lower temperatures when reduced metal has a catalytic effect as tin, e.g. (Epstein et al., 2010). In vacuum condition temperature of full conversion in Boudouard reaction is 600-700°C and CO_2 is usually fully transforms to CO at higher temperatures suitable for carboreduction of alumina and magnesia as an example. During carboreduction of light elements with complicated chemistry a series of more solid-gas reactions with intermediate suboxides and oxicarbides formation takes place.

All thermodynamic estimations were made using A. Roine HSC Chemistry Computer Code. According data presented in Fig.1 temperature of full conversion strongly increases with metal-oxygen bond strength as atom mass decreases and according Le Châtelier's principle can be reduced under vacuum conditions. In the other hand the lighter metals are more productive for hydrogen production per unit mass of a reduced metal. Also must be taken into account that despite the fact that thermolysis is free of CO, its reduction temperature is significantly higher than carboreduction temperature, and can be implement only at lower pressure of product gases that could be realized or at atmospheric pressure using significant amount of carrier gas, or at vacuum conditions. Figs.2b and 2c indicate that reaction temperature of ZnO carboreduction at atmospheric pressure is lower than ZnO thermolysis temperature at 1 mbar. Also it is usually impossible to prevent fully the reoxidation of reduced metals by pure oxygen. For today conversion achieved during ZnO thermal dissociation is 40% about (see section 4.1), whereas conversion of ZnO carbothermal reduction is 85-95% according XRD quantitative analysis (Wieckert et al. 2007; Vishnevetsky and Epstein, 2007). On the other hand, if carbon in Eq.1a was produced from bio source as charcoal, for example, its using can be considered as positive from economic and ecological point of view because product CO is an additional fuel and resulting CO2 will absorbed by plants, which will be used later for new charcoal production.

Besides advantages regarding high hydrolysis productivity of lighter elements with high metal-oxygen bond strength (Vishnevetsky et al. 2008, 2011a; Rosenband and Gany, 2010) their disadvantage is higher reduction temperature at atmospheric pressure that need vacuum conditions (compare ZnO and MgO carboreduction in Fig.2c, d) but also by-products formation during preheating of reactant mixture on the base of elements with higher valence, as shown in Fig.2e, f. Here it is possible to compare thermodynamics of carbothermic reduction of oxide with simple (ZnO, MgO) and complicated (Al2O3, B2O3) chemistry.

Another feature of carboreduction or splitting of oxides is output of CO or O_2 gases which usually contact with reduced deposited metals at the exit of the reactor that provokes reoxidation in backward reaction especially with oxygen. Possible way to avoid this future is the presence in the reaction zone of some amount of easily oxidizable element whose oxide is not gaseous but solid. Examples of equilibrium diagram for such reaction for Zn reduction, as an example, are presented in Fig.3

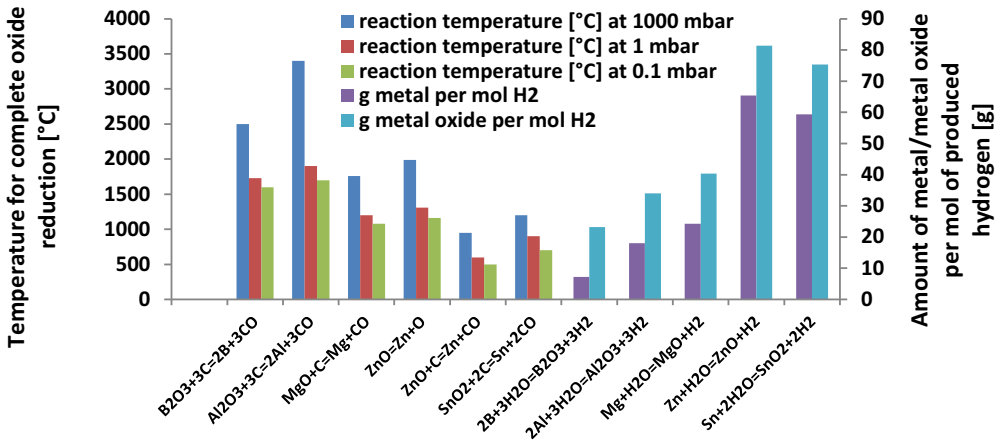

Fig.1: Thermodynamic estimation (Antti Roine HSC Chemistry Computer Code) of temperature for complete oxide reduction and productiveness of hydrolysis reaction

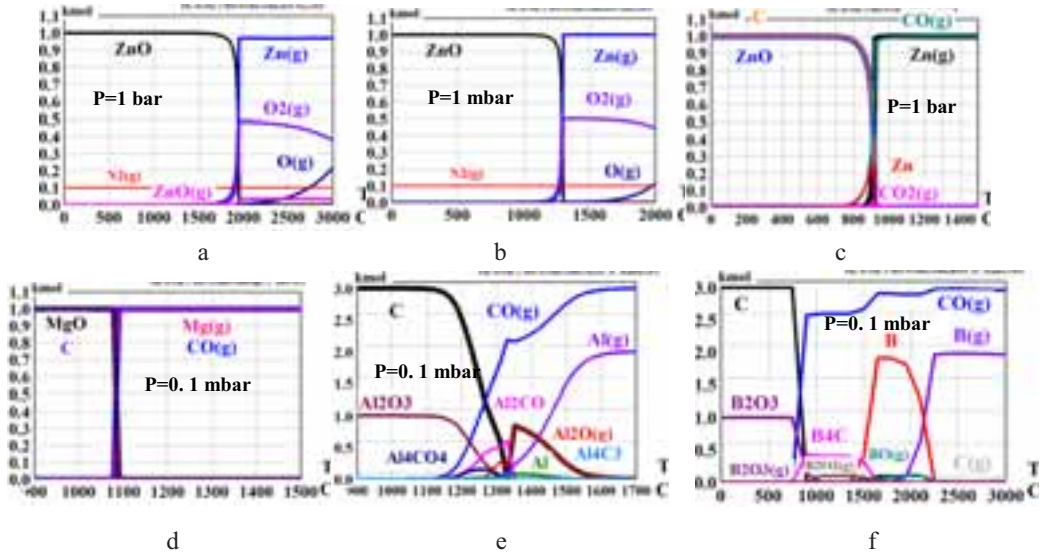

Fig.2: Equilibrium diagrams of (a) ZnO splitting at atmospheric pressure and (b) in vacuum; carboreduction of (c) ZnO at atmospheric pressure and (d) magnesia, (e) alumina, (f) boria in vacuum

As it is possible to conclude addition to the ZnO powder some amount of easily oxidizable element can significantly decrease reoxidation of reduced zinc. Of course, Molybdenum is not the best candidate for this but a small amount of light easily oxidizable element as boron, for example, can solve the problem catching the oxygen in the hot reaction zone made of a high temperature ceramic in a solar reactor. Equilibrium diagrams in Fig.3 (c, d) demonstrates that only 8.8 weight % of boron not only prevents Zn reoxidation but also significantly decreases temperature of zinc vapour production even at atmospheric pressure (compare Fig.3 c, d with thermal splitting in Fig.2 a, b). Bororeduction thermodynamically occurs at all temperatures and boron, unlike Mo, presents in the equilibrium diagram in oxidized form together with pure zinc also at low temperatures. In this case separation of reduced zinc from boron oxide can be realized during vaporization of Zn at temperatures higher than 900-1000°C at atmospheric pressure when boron oxide still liquid. If reaction proceeds at higher temperatures when Zn is in gas form, liquid B_2O_3 rests in a hot reaction zone. This process is free of CO_2 and could provide pure zinc solving the problem of Zn recombination because of instead gas product O_2 or CO there is liquid B_2O_3 which does not leave the hot reaction zone together with Zn. So following experiments of ZnO decomposition with small addition of pure boron powder could be very promising. Here it must be marked that such process is more suitable for recovering zinc oxidized in zinc-air fuel cells whereas for hydrogen production pure boron could be used itself. Boron oxide produced here can be used in different industries such as metallurgical, atomic energy, electronic and others or reduced to boron using solar energy.

Thermodynamic analysis indicates that bororeduction of magnesium oxide has no advantage over its carboreduction because of by-products as magnesium borides formation and a presence of boron oxides and suboxides in gaseous phase.

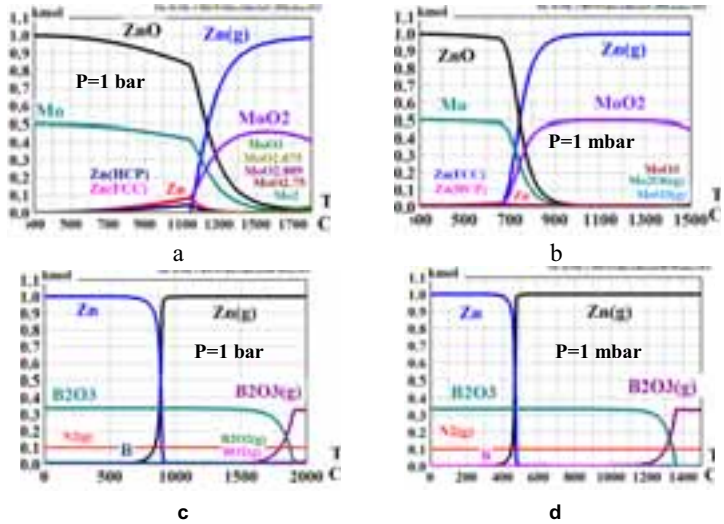

Fig. 3: Equilibrium diagrams of 1 mole ZnO decomposition at the presence of 0.5 mole of molybdenum: (a,b) and (c,d) 0.667 mole of boron at (a,c) atmospheric pressure; (b,d) in vacuum.

3. Experimental results and discussion

3.1. Morphology of carbo reduced metals depending on conditions of their vapors condensation or liquid product solidification

As it is possible to conclude from available results, metal hydrolysis can be realized using fine powder (Vishnevetsky et al. 2007, 2008, 2009, 2011a and Epstein et al, 2010) or liquid metal (Berman and Epstein, 2000). 10 μm conglomerates composed of micron and submicron particles have higher productivity compare with powder with larger particles or bubbling of liquid metal with water vapor.

Reduction of metals with boiling point higher than reaction temperatures provides product in a liquid phase which does not leave the reaction zone. Morphology of the reduced metal depends on the conditions of solidification (Vishnevetsky et al., 2010) and can present big conglomerates (Fig.4 a) or micron and submicron particles solidificated on the inert supports as 10 μm alumina particles, for example (Fig.4 b, c). Conversion of reduced tin was about 90%.

When reaction temperature is higher than boiling point of reduced metals in reaction conditions their morphology depends on quenching procedure. Quencher/cooler on the base of Cyclone with cold purge gas was used in SOLZINC pilot plant (Wieckert et al., 2007). It allows providing zinc powder with conglomerates till 10-20 μm composed of micron and submicron particles (Fig.5 a, b) and purity 85-95% as was mentioned above.

Morphology of metals deposited on surfaces of cold zone installed after hot reaction area (Figs.6, 7) strongly depends on temperature of a deposit site and on CO partial pressure at the deposit area. Deposits on water cooled surfaces usually represent powder with flakes deposited on sites with temperatures 50°C about or thin metallic films located on outer layers of a deposit or in a transition area from the hot to cold zone.

Fast cooling of Al vapors leads to formation of conglomerates composed of nanocrystallines, typical for flakes (Fig. 8 a, b) or composed of submicron spherical particles of Al (Fig. 8 c, d, e). Vacuum reactor (Fig. 7a) with water cooling deposit tube at 50-60°C was modified by adding the second option as uncooled deposit area to study vapour deposition at higher temperature for getting liquid reduced metal (Fig. 7b). Depending on insulation thickness and weather conditions temperature of the stainless steel tube can change from 340°C till 680°C. The best results with Al weight percent 97% according EDS were available in tests with hotter deposit site at temperature no higher than 460°C. Photo of metal plates (bright side contacting with the steel tube) collected from the lower cup and SEM image of outer matte side are presented in Fig. 8 f, g.

Maximal total weight conversion of reduced Al was 90% at avg./max. CO partial pressure 0.04/0.07 mbar and avg./max. reaction temperature 1525/1600°C. Increasing CO partial pressure till 0.2/0.4 mbar leads to conversion decreasing till 35-45%.

SEM images of magnesium deposited at sites with different temperatures are presented in Fig.9. Here also fast cooling of the magnesium vapor on the water cooled tube leads to formation of big conglomerates (Fig,9 a, b) composed by submicron crystals with 100% Mg contents (Fig.9 c). Deposit on transition area from hot to water cooled zone with temperature 200°C about composed by metallic flakes also arranged to spherical forms (Fig.9d). SEM image of inner layer with 100wt.% Mg contents deposited on place 6 in IH reactor (Fig.6b) with temperature 600°C about is presented in Fig.9e and the outer layer of the deposit from the same place with 70wt.% of Mg and 30% of MgO in Fig.9 f. Total conversion of Mg reduced in the solar vacuum reactor at avg./max P_{CO}=0.03/0.07 mbar and avg./max $t_{reaction}$=1535/1575°C was 90-95% related to reacted magnesia and 60-65% related to loaded magnesia because of significant amount of non-reacted sintered conglomerates (Fig. 10).

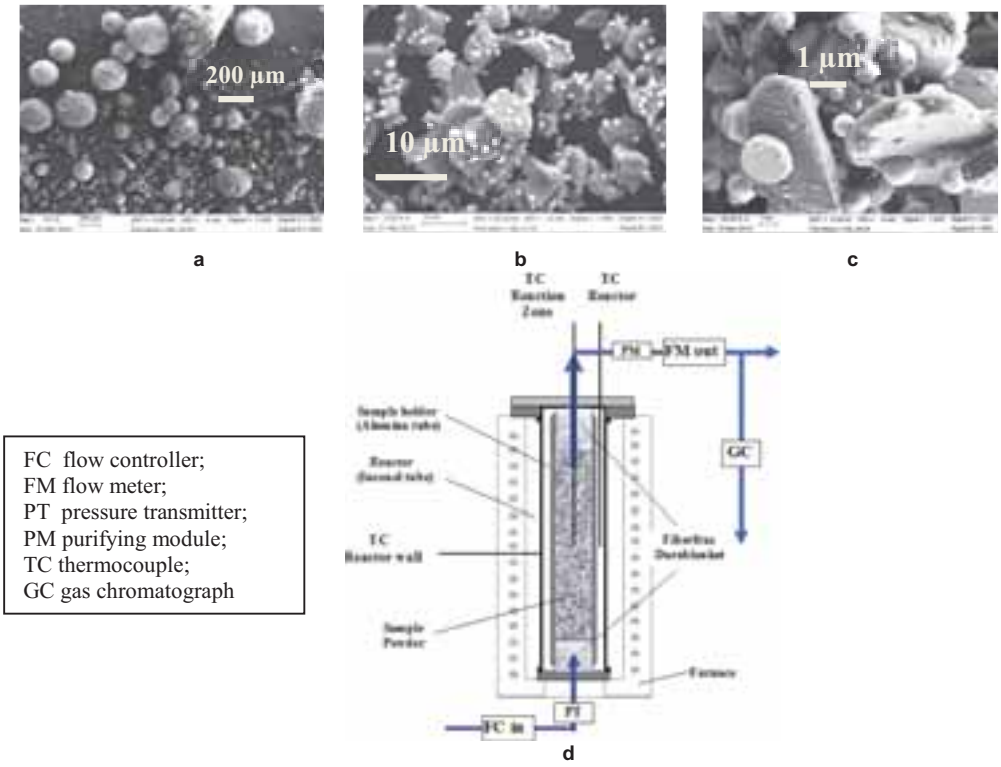

Fig. 4: Morphology of carbo reduced Sn: (a) stoichiometric ratio without inert support and (b, c) with 10 µm alumina powder as inert support loaded with reaction mixture into (d) tubular batch reactor

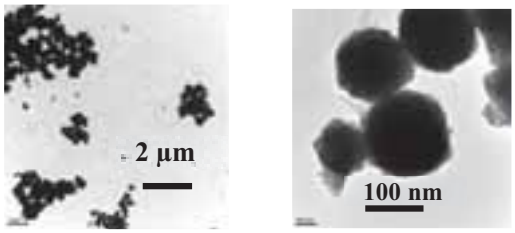

Fig.5: Morphology of SOLZINC powder (TEM images at different magnifications).

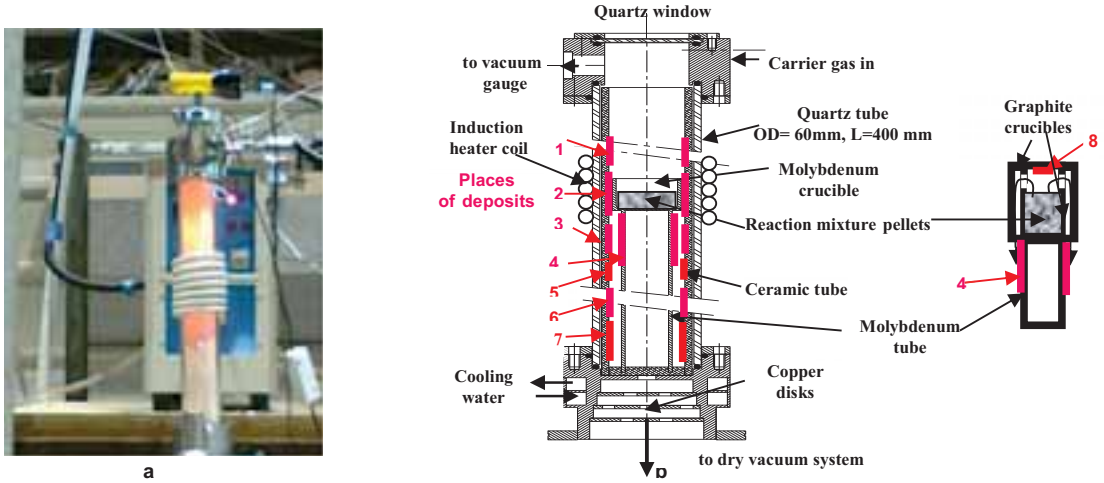

Fig.6: IH vacuum reactor: (a) photo of the Induction Heating (IH) vacuum reactor during operation; (b) principle schemes of non-solar IH setup (temperature in reaction crucibles 1400-1800°C and on deposit sites from 200°C to 1500°C)

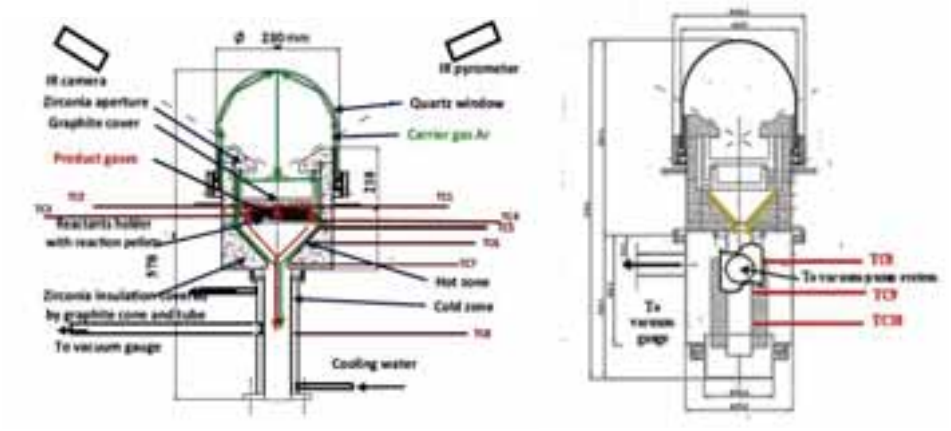

a b

Fig.7: Vacuum 10 kW solar reactors: schematic cross section of the solar reactor with (a) water cooling deposit site and (b) hotter deposit site

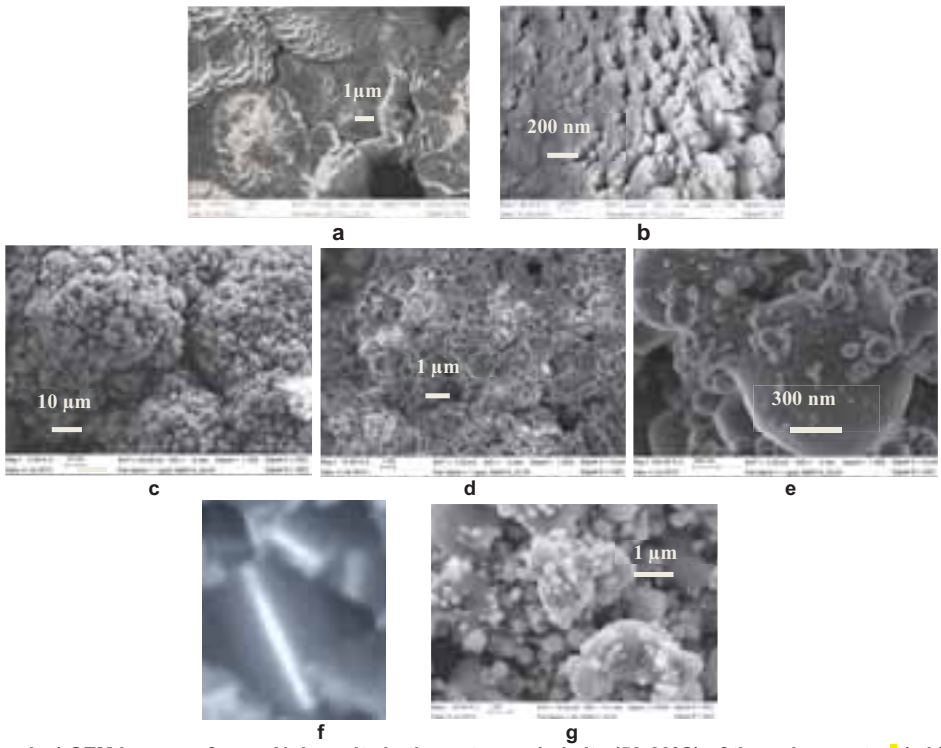

a b c d e f g

Fig. 8: (a, b, c, d, e) SEM images of pure Al deposits in the water cooled site (50-60°C) of the solar reactor: (a,b) Al flake ($P_{CO\ avg./max.}$=0.04/0.07 mbar); (c, d, e) thin Al film ($P_{CO\ avg./max.}$=0.064/0.18 mbar), ; (f) photo of bright side metal plates contacting with the not cooled stainless steel tube at temperature no higher 460◦C and (g) SEM image of its matte side with 95wt.% Al ($P_{CO\ avg./max.}$=0.05/0.125 mbar)

a b c

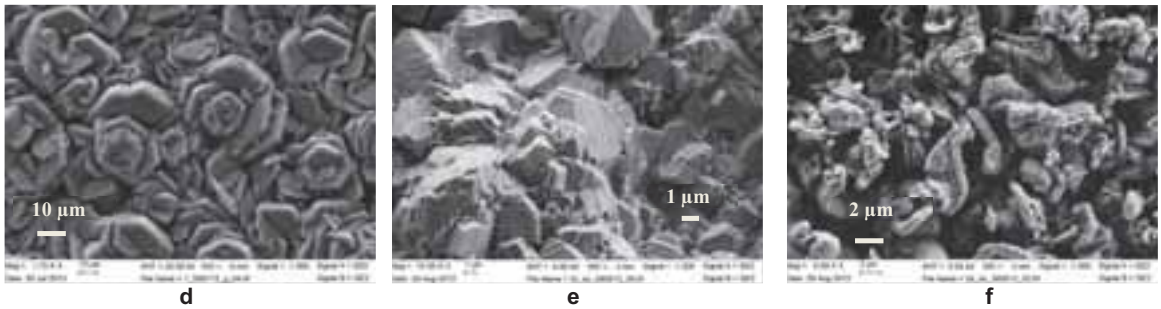

Fig.9: (a, b, c,) SEM images of pure Mg flakes deposited in the water cooled zone of solar reactor ($P_{CO\ avg./max.}$=0.03/0.07 mbar); (d) magnesium film deposited on transition area of solar reactor with temperature 200°C ($P_{CO\ avg./max.}$=0.019/0.055 mbar); (e) inner layer of the deposit with 100 wt.% Mg at low part of zirconia tube in IH reactor with temperature about 600°C ($P_{CO\ avg./max.}$=0.13/0.35 mbar); (f) outer layer of the deposit from the same place with 70 wt.% Mg and 30 wt.% MgO ($P_{CO\ avg./max.}$=0.24/0.5 mbar)

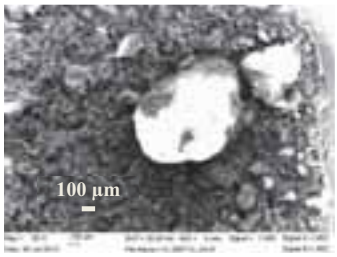

Fig.10: Non-reacted residual after magnesia carboreduction

3.2. Apparent activation energy as a function of CO partial pressure.

Unlike true activation energy of the reacting molecules apparent activation energy does not have such physical meaning and can depend on many parameters of a specific setup, including the partial pressure of participating gases that can be found in the literature (Ruiz and Delmon, 1992, as an example).

According LeChatelie principle CO partial pressure is a main parameter responsible for a rate of carboreduction reaction at given temperature. As it was mentioned above in Thermodynamics section such reactions realized as gas solid reactions where CO_2 is the main intermediate gas product that is usually fully transforms to CO at high temperatures suitable for carboreduction of alumina and magnesia.

When one of the main reaction product is gas, the rate of reaction can be estimated through its initial flow rate (Vishnevetsky and Epstein, 2009) related to amount of suitable elements in loaded reactants. Reaction rate of alumina and magnesia carboreduction was estimated as initial conversion rate through the CO release. The main measured parameters that must be taken into account are CO flow rate, reaction temperature and CO partial pressure (Fig.11). As it is possible to see, CO release in vacuum conditions presents in two peaks: CO in first peak is related to carbon and oxygen in sugar as a binder and in charcoal impurities and CO in second peak is a product of the reaction under consideration. First peak usually accompanied by small amount of H_2, CH_4 and CO_2 (Vishnevetsky et al., 2014). When carboreduction is carried out at atmospheric pressure at lower temperatures (ZnO and SnO_2 as an example) significant amount of CO_2 presents also in the main peak (Wieckert et al., 2007; Epstein et al., 2010) that also must be taken into account for initial conversion rate estimation. Starting of the second peak developing in vacuum condition is presented in Fig.11c, where τ_0 is time of the second peak onset and other τ_i (i=0,1, 2…) is times when CO flow rate develops. Conversion during any initial time period related to loaded moles of oxides can be calculated through release of CO and CO_2 (if any) using Eq.4 and initial conversion rate according Eq. 5 where initial amount of released oxygen atoms is divided to total amount of oxygen atoms in loaded oxide. Taking into account the short time difference between τ_i and τ_{i+1} related temperature and pressure can be simply averaged between τ_i and τ_{i+1}.

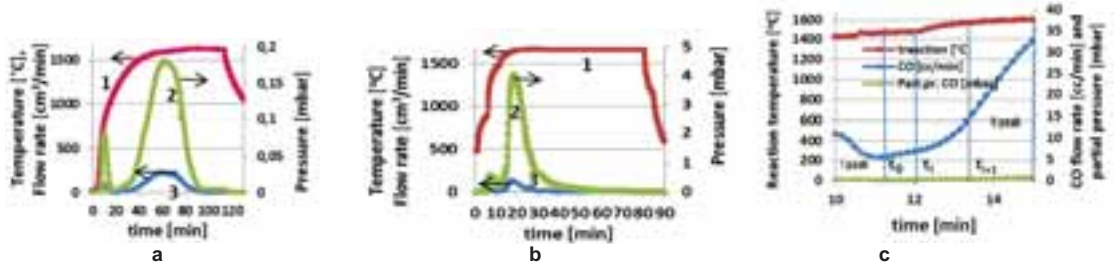

Fig.11: Main reaction parameters 1- Reaction temperature, 2 – CO partial pressure, 3 CO flow rate (alumina case): (a) batch solar reactor with slow preheating; (b) IH reactor with fast preheating; (c) second peak starting

$$Conversion = \frac{\text{mols CO} + 2 * \text{mols} CO_2}{y * \text{loaded mols } Me_x O_y} \quad \text{(eq.4)}$$

$$\frac{dConv._{initial}}{d\tau} = \frac{\int_{\tau_i}^{\tau_{i+1}} \left(F_{CO}(\tau) + 2 * F_{CO_2}(\tau)\right) d\tau}{22.4 * 10^3 * y * \text{loaded mols} Me_x O_y * (\tau_{i+1} - \tau_i)} \quad \text{(eq.5)}$$

Examples of Arrhenius plots for different averaged CO partial pressure are presented in Fig.12a. As it is possible to conclude higher pressure leads to higher apparent activation energy and higher pre-exponential factor which is proportional to the total number of reactants collisions. The last one confirms once again that oxide reduction with carbon has solid gas character (oxide with CO which is generated in Boudouard reaction of product CO_2 with loaded C). Apparent activation energy of alumina and magnesia carboreduction as function of CO partial pressure is presented in Fig.12b. It is possible to conclude that E_a sharply decreases at pressure less than 0.1 mbar and smoothly increases with higher pressure.

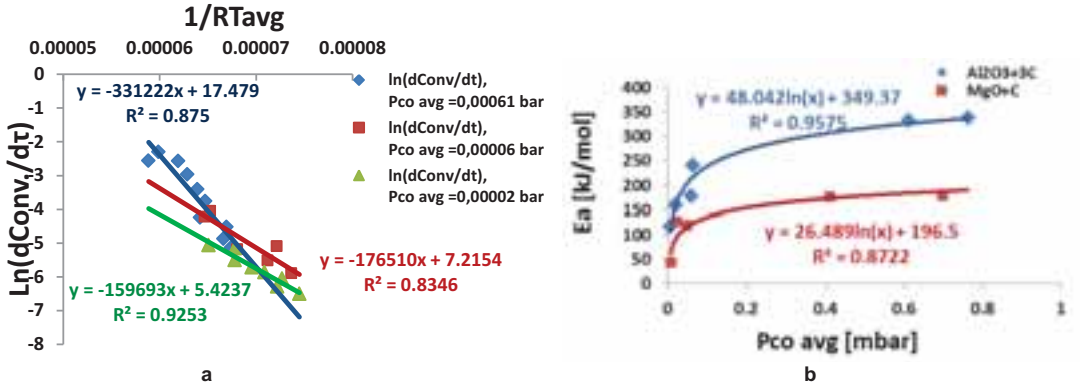

a b

Fig.12: (a) Examples of Arrhenius plots for different averaged CO partial pressure (alumina case) and (b) apparent activation energy as function of averaged CO partial pressure (alumina and magnesia case)

4. Current challenges of metal oxides thermal reduction and possible ways to overcome them

4.1 Recombination of Zn produced by thermal dissociation

As it is mentioned in Thermodynamics section, one of the main challenges of thermal splitting is recombination of reduced metals in backward reaction. The results achieved using laboratory rotating cavity reactor (Schunk et al., 2008) was Zn content in filtered particles at the range from 18.7 to 41.7 mole% of pure Zn and tests results of pilot scale reactor (Villasmil et al., 2014b) also provide only12–49% depending on the flow rate of Ar injected to a quench area. CNRS-PROMES reactor (Abanades et al., 2007) provide 70% Zn yield but using small cavity with ID=20 mm, whereas no pure zinc was produced when cavity ID was 30 mm.

ZnO thermal dissociation also was tested in the vacuum solar reactor with water cooling deposit site presented in Fig.7a by replacing all graphite parts to the same size parts made of a high density zirconia without cover that allows reaching 1800°C in reaction zone with loaded 15-20g ZnO pellets. Total maximal pressure was about 1 mbar and O_2 partial pressure is about 0.1 mbar. Full Zn conversion was no higher than 46% whereas according XRD quantitative analysis in some samples Zn wt.% reached 58-73%.

It was also demonstrated by Chambon at al.(2010) that in CNRS-PROMES vacuum reactor where 1g sample pellet was placed close to the refrigerator (on the distance of 4 cm only) it was possible to increase the mole fraction of reduced zinc from 10% to 75% decreasing total pressure from 20 kPa to 5 kPa.

After ZnO thermal dissociation tests in IH vacuum setup (Fig.6) with molybdenum crucible it was possible to get from deposit place 7 (with not very low temperature, about 300°C) bluish deposit with 96-100 wt. % Zn content that was about 75% of all Zn in loaded ZnO (FIg.13). Tests were run with 10g ZnO pellets at temperatures 1400-1500°C and partial pressure of oxygen was negligible, less than 0.004 mbar.

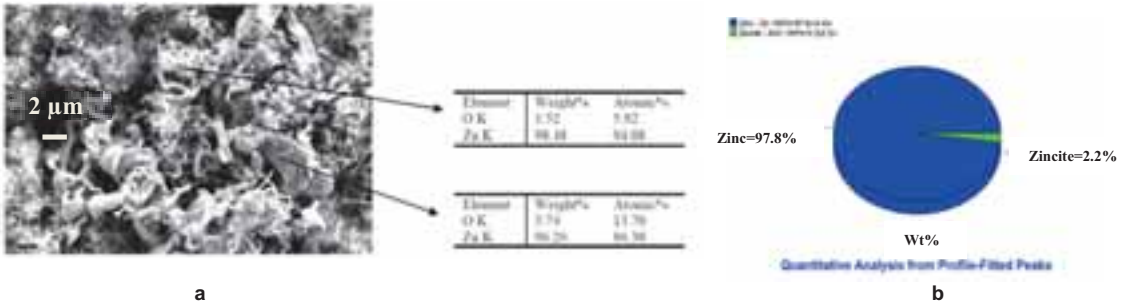

a b

Fig.13: (a) SEM image with EDS analysis and (b) XRD quantitative analysis of the bluish deposit at the low part of zirconia tube with 97.8 wt.% of Zn

At the same time the surfaces of molybdenum crucible and support tube were covered by MoO_2 with small addition of $Zn_2Mo_3O_8$. Zn recombination was not happened because of Mo cached the most of oxygen already in hot zone that is confirmed by thermodynamics (Fig. 3a, b) where instead gases Zn and O_2 (Fig.2a, b) only Zn(g) and MoO_2 are presented as reaction products.

4.2 By-product formation and possible oxide sintering at slow heating rate in batch reactors

Thermochemical batch reactor is the most convenient and safe for using concentrated solar energy especially in vacuum conditions. But the main challenge of batch reactor is relatively slow heating rate of the reactant loaded into a cold reactor. As it is possible to conclude from data in Fig.14a (details are presented by Vishnevetsky and Epstein (2015)), slower heating rate leads to reaction starting at lower temperature that provokes by-product formation in processes with complicated chemistry (Fig.2 e, f). As a result the reaction occurs at lower average temperature. Reaction time is longer (Fig.14b) that also could provoke possible reactant sintering and a significant amount of unreacted residual (Fig.10).

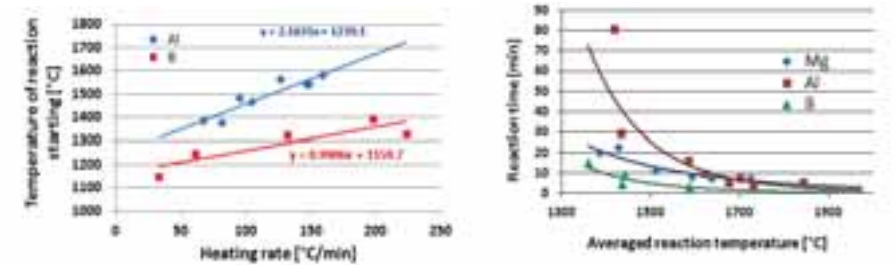

a b

Fig.14: (a) Temperature of reaction starting as function of the preheating rate and (b) reaction time at half the height of the CO peak as a function of the averaged reaction temperature.

Possible way to circumvent these problems is using a feeder reactor when reaction pellets doses by a vibrating vacuum feeder to a preheated vacuum reactor (Fig.15 a). Preheating and consumption times of reaction pellet dosed to the preheated reactor were estimated by Ben-Zvi (2015).The main results are presented in Fig.15b, c.

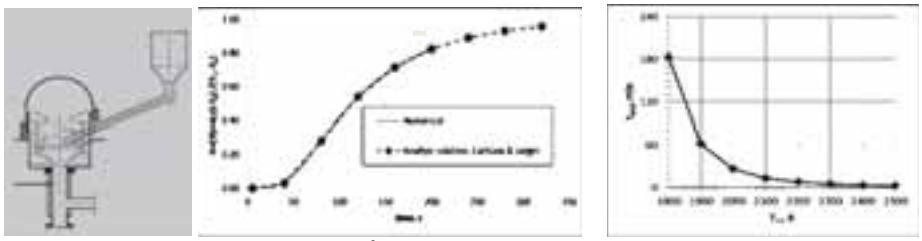

a b c

Fig. 15: (a) Solar reactor with vibrating vacuum feeder; (b) preheating and (c) consumption time of reactant pellets as function of reaction temperature (alumina case, P_{COavg}=8.17E-4 bar Ea ~337 kJ/mol)

According numerical and analytical estimation for alumina case, as an example, (Ben-Zvi, 2015) preheating time (Fig.15b) of 10 mm diameter spherical pellets is 5-6 min in the reactor with a feeder (1D transient conduction with initial pellet temperature T_0 =300K and prescribed outer temperature, T∞.) whereas in the batch reactor it is need one hour to reach the desirable temperature in the reaction zone (Fig.11a). In contrast to the preheating rate, pellets consumption time in a feeder reactor (Fig.15c) depends on temperature in the reaction zone and can be comparable with the pellets consumption time in a batch reactor (1-1.5 hours at 1600°C).

5. Conclusions

- Solar and non-solar setups developed during last 10-15 years for investigation of full reduction of metal oxides promising for solar thermochemical redox cycles for hydrogen production on demand are briefly described.
- Morphologies of reduced metals with different metal oxygen bond strength and boiling points were presented for various quenching conditions.
- Analyses of the purity of reduced metals with strong metal-oxygen bond strength as aluminum and magnesium show that metals with 95-100% purity and total conversion of reacted oxides at the level of 90-95% is possible when avg./max. CO partial pressure and temperature at the cold deposit area no higher than 0.07/0.2 mbar and 460°C in the case of aluminum and 0.1/0.35 mbar and 600°C in the case of magnesium. Rising of temperature and/or pressure results in recombination of reduced metals.
- Morphology of deposited aluminum and magnesium also strongly depends on deposit temperatures and can vary from conglomerates composed of submicron and nanocrystallines (50-60°C at water cooling deposit site), metallic flakes with spherical or flat micron and submicron particles (200°C about) to metallic plates (400-600°C).

- Apparent activation energy of alumina and magnesia carboreduction was estimated through an initial conversion rate as function of CO partial pressure. It was shown that this energy sharply decreases at pressure less than 0.1 mbar and smoothly increases with higher pressure.
- It was shown that significant recombination by oxygen of thermal dissociated Zn can be prevented by presence of an easily oxidizable element. Deposits with 98-99% pure zinc were available after tests with Mo crucible as sample holder in the IH reactor. It was demonstrated thermodynamically that small amount of boron could serve as the best easily oxidizable agent. Further confirmation in future experiments is required.
- It was experimentally confirmed that slow preheating rate in the batch vacuum reactor leads to decreasing temperature of reaction starting and averaged reaction temperature, resulting in undesirable by-product formation in forward reactions with complicated chemistry and possible sintering of oxides during longer preheating and reaction time. The possible way to prevent such disadvantage is using the reactor with a vacuum feeder. Preheating and consumption time of reactant pellets dosed to the hot reactor are estimated by a numerical simulation.
- Desirable following investigation of bororeduction of oxides with relatively heavy metal atoms and R&D of a vacuum reactor with vibrating vacuum feeder are proposed.

Acknowledgements

Invaluable assistance of my colleges from Solar Research Facilities Unit and Chemical Research Support, as well as the EC/FP7/ENEXAL project for financing is gratefully acknowledged.

References

Abanades, S, Patrice Charvin, P., Flamant, G., 2007. Design and simulation of a solar chemical reactor for the thermal reduction of metal oxides: Case study of zinc oxide dissociation, Chemical Engineering Science 62, 6323 – 6333.

Abanades, S., Charvin, P.,Lemort,F.,Flamant,G.,2008. Novel two-step SnO_2/SnO water-splitting cycle for solar thermochemical production of hydrogen. International JournalofHydrogenEnergy33(21),6021–6030.

Adinberg R., Epstein M., 2004. Experimental study of solar reactors for carboreduction of zinc oxide, Energy 29 , 757–769.

Ben-Zvi, R., 2013. Numerical simulation and experimental validation of a solar metal oxide reduction system under vacuum. Sol. Energy 98, 81–189.

Ben-Zvi, R., 2015. Transient one-dimensional reactive pellet simulation, Sol. Energy 115, 10–15.

Berman, A., and Epstein, M., 1999. The kinetic model for carboreduction of zinc oxide J. Phys. IV France 9, Pr3-320

Berman, A., and Epstein, M., 2000. The kinetics of hydrogen in the oxidation of liquid zinc with water vapor, Int. J. Hydrogen Energy, 25, pp. 957–967.

Byung-Su Kim, Jae-Min Yoo, Jin-Tae Park and Jae-Chun Lee, 2006. A kinetic study of the carbothermic reduction of zinc oxide with various additives. Materials Transactions, Vol. 47, No. 9, 2421 - 2426

Chambon, M., Abanades, S., Flamant, G., 2010. Solar thermal reduction of ZnO and SnO_2: Characterization of the recombination reaction with O_2, Chemical Engineering Science 65, 3671–3680.

Epstein, M., Olalde, G., Santén, S., Steinfeld, A., Wieckert, C., 2008. Towards the industrial solar carbothermal production of Zinc, J. Sol. Energy Eng., 130, 014505-1-4.

Epstein, M., Vishnevetsky, I., Berman A., 2010. The SnO2/Sn carbothermic cycle for splitting water and production of hydrogen, ASME Journal of Solar Energy Engineering 132, 031007–1–7.

Fletcher, E.A., 2001. Solarthermal processing: a review. J. Solar Energy Eng. 123, 63–74.

Frommherz, U., Osinga,T., Steinfeld, A., Wieckert, C., 2002. Experimental investigation of the solar carbothermic reduction of ZnO using two cavity solar reactor. http://www.pre.ethz.ch/publications/0_pdf/sci_rep/solzinc_Annex2002b.pdf

Haueter, P., Moeller, S., Palumbo, R., and Steinfeld, A., 1999. The production of zinc by thermal dissociation of zinc oxide – solar chemical reactor design, Solar Energy 67, 161–167. Hydrosol project, http://160.40.15.244/hydrosol/index.html

Kodama, T., 2003. High-temperature solar chemistry for converting solar heat to chemical fuels. Progress in Energy and Combustion Science 29, 567–597.

Kogan, A., and Kogan, M., 2002. The Tornado Flow Configuration—An effective method for screening of a solar reactor window, ASME J. Sol. Energy Eng., 124(3), pp. 206–214.

Konstandopoulos, A.G., Agrofiotis, C., 2006. Hydrosol : Advanced monolithic reactors for hydrogen generation from solar water splitting. Revue des Energies Renouvelables. 9, 121 – 126.

Meier A., STAGE-STE Presentation of Paul Scherrer Institute (PSI) Solar Technology Laboratory, www.stage-ste.eu

Muhich Christopher L., Ehrhart Brian D., Al-Shankiti Ibraheam, Ward Barbara J., Musgrave Charles B., Weimer Alan W., 2015. A review and perspective of efficient hydrogen generation via solar thermal water splitting. WIREs Energy Environ. doi: 10.1002/wene.174 (in press).

Osinga, T., Frommherz, U., Steinfeld, A., Wieckert, C., 2004a, Experimental investigation of the solar carbothermic reduction of ZnO using a two-cavity solar reactor, J. Sol. Energy Eng 126, 633-637.

Osinga,T., Olalde, G and Steinfeld, A., 2004b. Solar carbothermal reduction of ZnO: shrinking packed-bed reactor modeling and experimental validation. Ind. Eng. Chem. Res. 43, 7981-7988.

Roeb M., Neises M., Monnerie N., Call F., Simon H., Sattler C., Schmücker M. and Pitz-Paal R., 2012. Materials-related aspects of thermochemical water and carbon dioxide splitting: A Review. Materials, 5, 2015-2054.

Rosenband, V., Gany A., 2010. Application of activated aluminum powder for generation of hydrogen from water, International Journal of Hydrogen Energy, 35 , 10898-10904.

Ruis P. and Delmon B. (Eds), 1992. New developments in selective oxidation by heterogeneous catalysis. Studies in surface science and catalysis, 72, 123-132.

Scheffe J.R. and Steinfeld A., 2014. Oxygen exchange materials for solar thermochemical splitting of H_2O and CO_2: a review, Materials Today , 17(7), 341-348.

Schunk, L. O., Haeberling, P., Wepf, S., Wuillemin, D., Meier, A., Steinfeld, A., 2008. A receiver-reactor for the solar thermal dissociation of zinc oxide, J. Sol. Energy Eng., 130, 021009-1-6.

Steinfeld, A., Palumbo, R., 2001. Solar thermochemical process technology. In: Meyers, R.A. (Ed.), Encyclopedia of Physical Science and Technology, 15. Academic Press, pp. 237–256.

Steinfeld, A., 2005. Solar thermochemical production of hydrogen—a review. Solar Energy 78, 603–615.

Villasmil, W, Meier, A. Steinfeld, A., 2014a. Dynamic modeling of a solar reactor for zinc oxide thermal dissociation and experimental validation using IR thermography, J. Sol. Energy Eng. 136, 010901-1-11.

Villasmil, W., Brkic, M., Wuillemin, D., Meier, A., Steinfeld, A., 2014b. Pilot scale demonstration of a 100- kWth solar thermochemical plant for the thermal dissociation of ZnO, J. Sol.Energy Eng.136, 011016-1-11.

Vishnevetsky, I., Epstein, M., Rubin R., 2005. Simulation of thermal and chemical processes in annular layer of ZnO–C mixtures. J. Solar Energy Eng. 127, 401-412.

Vishnevetsky, I., Epstein, M., Ben-Zvi, R., and Rubin, R., 2006. Feasibility study on nonwindowed solar reactor: ZnO carboreduction as an example, Sol. Energy, 80(10), pp. 1363–1375.

Vishnevetsky, I., Epstein, M., 2007, Production of hydrogen from solar zinc in steam atmosphere, International Journal of Hydrogen Energy, 32, pp. 2791–2802

Vishnevetsky, I., Epstein, M., Abu-Hamed, T., Karni, J., 2008. Boron hydrolysis at moderate temperatures: first step to solar fuel cycle for transportation, J. Sol. Energy Eng. 130, 014506 1-5.

Vishnevetsky, I., Epstein, M., 2009, Tin as a possible candidate for solar thermochemical redox process for hydrogen production, ASME Journal of Solar Energy Engineering 131, 021007–1-8

Vishnevetsky, I., Epstein, M., Feldman Y., 2010. Preventing conglomeration of reduced fine powder in solar thermochemical redox cycles based on metals with low melting and high boiling points, Proceedings of the Mechanical Engineering Congress & Exposition, November 12-18, Vancouver, British Columbia, Canada, paper IMECE2010-38097.

Vishnevetsky, I., Berman, A., Epstein, M., 2011a. Features of solar thermochemical redox cycles for hydrogen production from water as a function of reactants' main characteristics, International Journal of Hydrogen Energy 36, Issue 4, 2817–2830.

Vishnevetsky, I., Epstein, M., 2011b. Metal oxides reduction in vacuum: setup development and first experimental results. Proceeding of 17 International Symposium Solar PACES; September 20–23, Granada, Spain, paper 23698.

Vishnevetsky, I., Ben-Zvi, R., Epstein, M., 2012. Solar metal oxide reduction under vacuum, experimental investigation of the alumina case, Proceeding of 18 International Symposium Solar PACES; September 11–14, Marrakesh , Morocco

Vishnevetsky, I., Ben-Zvi, R., Epstein, M., Barak, S., Rubin, R., 2013. Solar carboreduction of alumina under vacuum, JOM. J. Min. Met. Mater. Soc. (TMS) 65, 1721–1732.

Vishnevetsky, I., Epstein, M., Rubin, R., 2014. Solar carboreduction of alumina under vacuum, Energy Procedia 49, 2059–2069 (Proceedings of the SolarPACES 2013 International Conference)

Vishnevetsky, I., Epstein, M., 2015. Solar carbothermic reduction of alumina, magnesia and boria under vacuum, Solar Energy 111, 236-251.

Wieckert, C., Palumbo, R, Frommherz, U., 2004, A two-cavity reactor for solar chemical processes: heat transfer model and application to carbothermic reduction of ZnO, Energy 29, 771–787 (SolarPACES 2002).

Wieckert, C., Frommherz, U., Kräupl, S., Guillot, E., Olalde, G., Epstein, M.,. Santén, S., Osinga, T., Steinfeld, A., 2007. A 300 kW solar chemical pilot plant for the carbothermic production of zinc, J. Sol. Energy Eng. 129(2), pp. 190-196.